Anal. Chem. **2009,** *81,* 7003–7008

Electrocatalytic Activity of Pd−Co Bimetallic Mixtures for Formic Acid Oxidation Studied by Scanning Electrochemical Microscopy

Changhoon Jung, Carlos M. Sánchez-Sánchez, Cheng-Lan Lin, Joaquín Rodríguez-López, and Allen J. Bard*

Center for Electrochemistry, Department of Chemistry and Biochemistry, Center for Nano-and Molecular Science and Technology, The University of Texas at Austin, Austin, Texas 78712

The electrochemical oxidation of formic acid was studied by the tip generation-substrate collection (TG-SC) mode of scanning electrochemical microscopy (SECM), extending the number of applications of SECM in electrocatalysis. Formic acid was generated at a Hg on Au ultramicroelectrode (UME) tip by reduction of CO_2 in a 0.1 M $KHCO_3$ solution saturated with this gas. The electrocatalytic activity of different Pd−Co bimetallic compositions was evaluated using a Pd−Co electrocatalyst array formed by spots deposited onto glassy carbon (GC) as a SECM substrate. The SECM tip, which generated a constant formic acid flux, was scanned above the array and the oxidation current generated when formic acid was collected by active electrocatalytic spots was displayed as a function of tip position. This generated a SECM image that showed the electrocatalytic activity of each spot. SECM screening identified $Pd_{50}Co_{50}$ (Pd/Co = 50:50, atomic ratio) as a better electrocatalyst toward the formic acid oxidation than pure Pd or Pt in 0.1 M $KHCO_3$ solution and this result was confirmed by cyclic voltammetry. Positive feedback was observed for the most active compositions of Pd−Co which suggests fast reaction kinetics and chemical reversibility during the oxidation of formic acid to CO_2. Moreover this feedback increases the contrast between active and non-active spots in this imaging mode.

Low temperature fuel cells, such as direct methanol fuel cells (DMFCs) and direct formic acid fuel cells (DFAFCs), are attractive as clean power sources for portable electronic devices. In the last few decades, platinum-based electrocatalysts have been employed for the oxidation of the respective fuel at the anode of these low temperature fuel cells.[1,2] Much interest has been paid, however, to the development of alternative electrocatalysts to platinum; this is mainly due to its high cost, limited availability for scale-up, and its rapid loss of activity caused by poisoning species generated during the oxidation process, such as adsorbed CO.[3−9] One solution is to add a second metal to platinum to enhance the activity. Pt/Ru, Pt/Pd, Pt/Au and Pt/Pb have recently proven to be more efficient catalysts for the oxidation of formic acid in DFAFCs.[10] Palladium is known to be a better electrocatalyst for formic acid oxidation than platinum, and has shown better performance as well as stronger resistance to CO poisoning in sulfuric acid solution.[11−13] The onset potential for formic acid oxidation on Pd electrodes is about 400 mV more negative than that on Pt electrodes, and the oxidation current due to formic acid oxidation is similar in the forward and backward sweep direction when evaluated by cyclic voltammetry.[11] The activity of the Pd catalyst, however, decreases with the cell operation time, and for this reason, a few papers have recently reported different Pd−Co bimetallic alloys that improve the palladium electrocatalytic activity and stability for formic acid oxidation.[14,15] Electrochemical and spectroscopic techniques, such as cyclic voltammetry,[1,2] rotating disk electrode (RDE) studies,[4,16] and Fourier transform infrared spectroscopy (FT-IR),[17−19] have been used to study relevant aspects of electrocatalysts, such as their activity and their resistance to poisoning during formic acid oxidation.

* To whom correspondence should be addressed. E-mail: ajbard@mail.utexas.edu. Phone: 1-512-471-3761. Fax: 1-512-471-0088.

(1) Feliu, J. M.; Herrero, E. *Handbook of Fuel Cells - Fundamentals, Technology, and Applications*; Vielstich, W., Lamm, A., Gasteiger, H. A., Eds.; Wiley & Sons, Ltd.: Chichester, 2003.
(2) Markovic, N. M.; Ross, P. N. *Sur. Sci. Rep.* **2002**, *45*, 121–229.
(3) Babu, P. K.; Tong, Y. Y.; Kim, H. S.; Wieckowski, A. *J. Electroanal. Chem.* **2002**, *524*, 157–164.
(4) Rice, C.; Ha, S.; Masel, R. I.; Wieckowski, A. *J. Power Sources* **2003**, *115*, 229–235.
(5) Iwasita, T.; Hoster, H.; John-Anacker, A.; Lin, W. F.; Vielstich, W. *Langmuir* **2000**, *16*, 522–529.
(6) Baldauf, M.; Kolb, D. M. *J. Phys. Chem.* **1996**, *100*, 11375–11381.
(7) Marković, N. M.; Gasteiger, H. A.; Ross, P. N., Jr.; Jiang, X.; Villegas, I.; Weaver, M. J. *Electrochim. Acta* **1995**, *40*, 91–98.
(8) Climent, V.; Herrero, E.; Feliu, J. M. *Electrochim. Acta* **1998**, *44*, 1403–1414.
(9) Napporn, W. T.; Laborde, H.; Lager, J.-M.; Lamy, C. *J. Electroanal. Chem.* **1996**, *404*, 153–159.
(10) Yu, X.; Pickup, P. G. *J. Power Sources* **2008**, *182*, 124–132.
(11) Liu, Z.; Hong, L.; Tham, M. P.; Lim, T. H.; Jiang, H. *J. Power Sources* **2006**, *161*, 831–835.
(12) Larsen, R.; Zakzeski, J.; Masel, R. I. *Electrochem. Solid State Lett.* **2005**, *8*, A291−A293.
(13) Ha, S.; Larsen, R.; Zhu, Y.; Masel, R. I. *Fuel Cells* **2004**, *4*, 337–343.
(14) Wang, X.; Xia, Y. *Electrochem. Commun.* **2008**, *10*, 1644–1646.
(15) Wang, R.; Liao, S.; Ji, S. *J. Power Sources* **2008**, *180*, 205–208.
(16) Morimoto, Y.; Yeager, E. B. *J. Electroanal. Chem.* **1998**, *444*, 95–100.
(17) Samjeske, G.; Miki, A.; Ye, S.; Osawa, M. *J. Phys. Chem. B* **2006**, *110*, 16559–16566.
(18) Iwasita, T.; Nart, F. C.; Lopez, B.; Vielstich, W. *Electrochim. Acta* **1992**, *37*, 2361–2367.
(19) Chen, Y.-X.; Heinen, M.; Jusys, Z.; Behm, R. J. *Langmuir* **2006**, *22*, 10399–10408.

10.1021/ac901096h CCC: $40.75
Published on Web 07/23/2009

Recent investigations carried out in our group have demonstrated the utility of SECM as a rapid and high throughput technique for screening electrocatalysts for processes such as the oxygen reduction reaction (ORR)[20,21] and the oxygen evolution reaction (OER).[22] In this work, we extend the use of the tip generation-substrate collection (TG-SC) mode of the SECM for the screening of anodic electrocatalysts for formic acid oxidation with possible applications in DFAFCs. The studies presented here are intended to assess the electrocatalytic activity for formic acid oxidation of different compositions of Pd−Co mixtures in 0.1 M $KHCO_3$ solution. This work increases the scope and demonstrates the feasibility of TG-SC mode of the SECM to study anodic electrocatalytic processes.

EXPERIMENTAL SECTION

Chemicals. $(NH_4)_2PdCl_4$ 99.998%, $Co(NO_3)_2(H_2O)_6$ 99.999%, H_2PtCl_6 99.998% and glycerol (all Alfa Aesar, Ward Hill, MA), HNO_3 65% and HCOOH 97% (both Acros Organics, NJ), $KHCO_3$ 99.5% (Fisher, Fair Lawn, NJ), $Hg_2(NO_3)_2$ (Fluka) and sulfuric acid 94%−98% (trace metal grade, Fisher Scientific, Canada) were used as received. Small squares (1 mm thick, 15 × 15 mm^2) of glassy carbon (GC) were made from larger plates (1 mm thick, 50 × 50 mm^2, Alfa Aesar, Ward Hill, MA) and used as substrates. Reagent solutions were prepared using Milli-Q water (Millipore Co., Bedford, MA).

Preparation of Electrocatalyst Arrays. The detailed method for the preparation of the arrays through picoliter dispensing is described in a previous paper.[20] Briefly, precursor solutions of 0.3 M $(NH_4)_2PdCl_4$, $Co(NO_3)_2(H_2O)_6$, or H_2PtCl_6 were prepared using water-glycerol (3/1, v/v) as the solvent. The precursor solutions were deposited onto GC substrate as liquid spots with different volume ratios by a piezo-based microarray dispenser (MicroJet AB-01−60, MicroFab, Plano, TX). The distance between each spot was 500 μm. The array was dried under Ar at 150 °C overnight and then reduced with H_2 at 350 °C for 1 h in a tube furnace. For the arrays used in this study, the total number of dispensed drops and the molar concentration of the precursor solutions was the same, assuring that the atomic ratios of the different spots corresponded to the volumes used in each spot.

Preparation of the Hg on Au Ultramicroelectrode (UME). A Hg thin film was electrodeposited onto a Au UME (25 μm dia., RG = 10) in a deoxygenated 5 mM $Hg_2(NO_3)_2$, 0.5% HNO_3, and 0.1 M KNO_3 solution at −0.1 V (vs Ag/AgCl) for 100 s.[23,24] The Au UME was fabricated by heat-sealing a Au wire (25 μm dia.) in a borosilicate glass capillary under vacuum. The capillary glass was then polished to reveal the Au surface and sharpened using sand paper. The UME was further polished using alumina powders (particle size: 1.0, 0.3, and 0.05 μm) on polishing cloth to obtain a smooth Au surface before the Hg deposition.

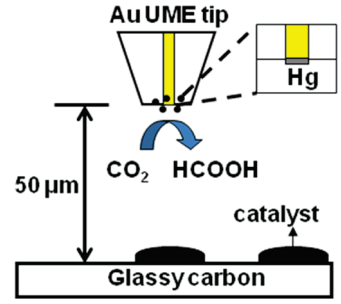

Figure 1. Operation scheme of the TG-SC mode of the SECM for formic acid oxidation electrocatalyst screening.

Scanning Electrochemical Microscopy. Figure 1 shows the operational scheme of the TG-SC mode of the SECM employed for the study of formic acid oxidation on electrocatalyst arrays in a 0.1 M $KHCO_3$ solution saturated with CO_2 gas (pH = 8). A CHI model 900B SECM (CH Instruments, Austin, TX) was employed to carry out the experiments at room temperature in a four-electrode arrangement. The SECM probe was a Au UME tip (25 μm diameter) modified with an electrodeposited Hg thin layer, and a constant potential (E_{tip} = (−1.6) to (−2.0) V) was applied to this tip to generate a constant flux of formic acid from the reduction of CO_2 dissolved in the electrolyte. The tilt of the substrate electrode was corrected until an acceptable vertical to horizontal displacement was achieved, that is, $\Delta z/\Delta x$(or Δy) $\leq$ 1.5 μm/mm. The Hg on Au UME generator tip was brought to a close and constant distance above the electrocatalyst array (≈50 μm) and scanned in the *X-Y* plane. The array substrate was held at a constant potential in the active region for the formic acid oxidation. In this way, the SECM images obtained provide a rapid method of evaluating the electrocatalytic activity of the spots present in the array, since these images represent the oxidation current produced at the substrate as a function of the tip generator position. A CO_2 blanket was maintained over the 0.1 M $KHCO_3$ solution during the experiment to keep the solution free from atmospheric oxygen and saturated with CO_2. A salt bridge-connected Ag/AgCl electrode and a Au wire were used as the reference and the counter electrode, respectively. All potentials reported here are referred to the Ag/AgCl reference electrode.

Linear Sweep Voltammetry (LSV). LSV was employed in a conventional three-electrode configuration using a Hg on Au UME (25 μm diameter), Ag/AgCl, and platinum wire as a working, reference, and auxiliary electrodes, respectively. The electrolyte was an aqueous solution containing 0.1 M $KHCO_3$ purged with either Ar or CO_2 gas. The scan rate was 50 mV/s.

Chronoamperometry. A constant potential in the range of −1.6 to −2.0 V was applied to the Hg on Au UME (25 μm diameter) using an Ag/AgCl and a platinum wire as a reference and auxiliary electrodes, respectively. The electrolyte was an aqueous solution containing 0.1 M $KHCO_3$. The electrolyte was purged with CO_2 for 1000 s, and then was purged with Ar during the experiments.

Cyclic voltammetry (CV). CV was employed in a conventional three-electrode system for larger area electrodes to compare the behavior of the successful Pd−Co electrocatalysts found after

(20) Fernández, J. L.; Walsh, D. A.; Bard, A. J. *J. Am. Chem. Soc.* **2005**, *127*, 357–365.
(21) Lin, C. L.; Sanchez-Sanchez, C. M.; Bard, A. J. *Electrochem. Solid State Lett.* **2008**, *11*, B136–B139.
(22) Minguzzi, A.; Alpuche-Aviles, M. A.; Rodríguez-López, J.; Rondinini, S.; Bard, A. J. *Anal. Chem.* **2008**, *80*, 4055–4064.
(23) Mauzeroll, J.; Hueske, E. A.; Bard, A. J. *Anal. Chem.* **2003**, *75*, 3880–3889.
(24) Sánchez-Sánchez, C. M.; Rodriguez-Lopez, J.; Bard, A. J. *Anal. Chem.* **2008**, *80*, 3254–3260.

SECM screening with Pt and Pd electrodes. Three independent arrays of 25 spots with the same format as the arrays used in SECM screening were made solely for Pt, Pd and $Pd_{50}Co_{50}$ respectively and were used as the working electrode. The reference and counter electrodes used were the same as in the SECM experiments. The electrolyte was an aqueous solution containing 0.1 M $KHCO_3$ with 10 mM HCOOH (pH = 7.3) and was purged with Ar for at least 15 min before the experiments. The scan rate was 50 mV/s.

RESULTS AND DISCUSSION

CO_2 Reduction at a Hg on Au UME. The electrochemical reduction of CO_2 in aqueous media can produce different products depending on the metal employed as the electrode material. Hg is one of the few metals that selectively produce formic acid as the main product of electrochemical CO_2 reduction.[25−27] For the study of formic acid oxidation at an electrocatalyst array using the TG-SC mode of the SECM, a steady-state generation of formic acid from CO_2 reduction at an UME probe is required. Figure 2(a) shows the cathodic linear sweep voltammetry of a Hg on Au UME in 0.1 M $KHCO_3$ solution with and without CO_2 saturation. The onset potential of CO_2 reduction was observed at −0.5 V and significant proton reduction was found beyond −2.0 V limiting the potential window. To have effective CO_2 reduction current at the UME without significant proton reduction, a potential range between −1.6 and −2.0 V was chosen. Figure 2(b) shows the cathodic current responses of a Hg on Au UME at different potentials, first with CO_2 saturation and then with Ar purging for 1000 s. Stable and reproducible CO_2 reduction currents at the UME were observed when the applied potentials were between −1.6 and −1.9 V. The CO_2 reduction efficiency at the Hg on Au UME can be estimated by following eq 1:

$$CO_2 \text{ reduction efficiency} = \frac{(i_t - i_{H^+})}{i_t} \times 100\% \qquad (1)$$

where i_t is the total cathodic current, which consists of the currents of both CO_2 and proton reduction in CO_2 saturated solution, and i_{H^+} is the proton reduction current at the UME in the absence of CO_2. The calculated CO_2 reduction efficiency was higher than 70% at all applied potentials (see Figure 3). It is noteworthy that the CO_2 reduction found at −1.9 V has a higher efficiency (92%) than at other lower potentials, and this is consistent with a previously reported value.[27] The Hg on Au UME shows stable and highly efficient formic acid generation ability for reducing CO_2 in 0.1 M $KHCO_3$ solution, thus proving its utility as a suitable probe in the TG-SC mode of the SECM for formic acid oxidation studies. O_2 interference during formic acid generation at the tip and formic acid oxidation at the studied electrocatalysts is avoided by the purging effect of CO_2 or Ar.

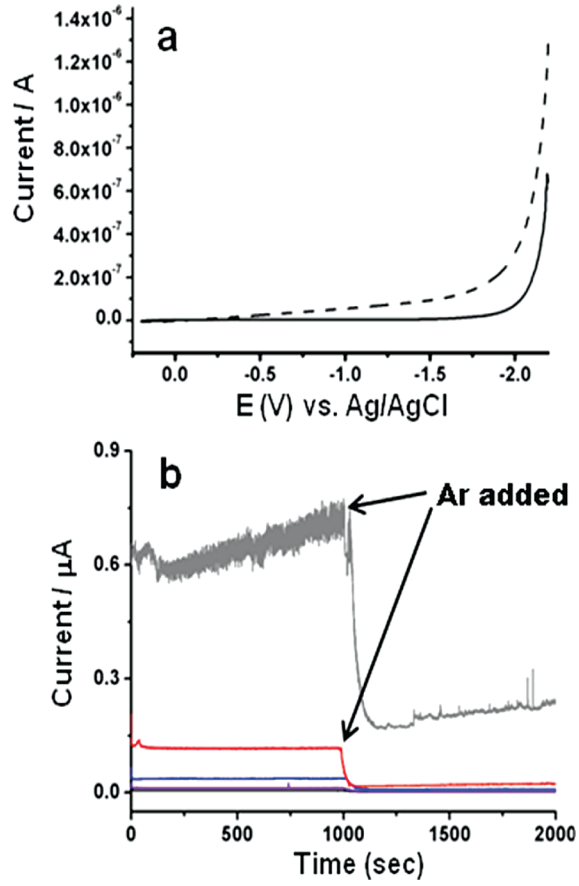

Figure 2. (a) Linear sweep voltammograms at Hg on Au UME in a CO_2 saturated electrolyte for CO_2 reduction (dashed line) and in an Ar purged electrolyte for H^+ reduction (solid line). The electrolyte was a 0.1 M $KHCO_3$ solution. The scan rate was 50 mV/s. (b) Chrono-amperometric curves of CO_2 reduction on a Hg on Au UME at −2.0 V (gray), −1.9 V (red), −1.8 V (blue), −1.7 V (purple), and −1.6 V (black). The electrolyte was purged with CO_2 in the time period from 0 to 1000 s, and then was purged with Ar.

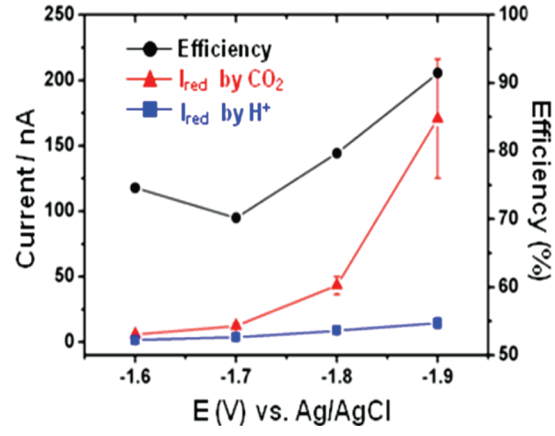

Figure 3. Total cathodic current (i_t, red triangles), the proton reduction current (i_{H^+}, blue squares), and the calculated CO_2 reduction efficiency (black circles) at a Hg on Au UME in 0.1 M $KHCO_3$ solution.

SECM Activity Imaging of Formic Acid Oxidation on a Pd−Co Electrocatalyst Array. The TG-SC mode of the SECM was employed to study the formic acid oxidation activity of a series of Pd−Co electrocatalysts with different Pd to Co atomic ratios.

(25) Jitaru, M.; Lowy, D. A.; Toma, M.; Toma, B. C.; Oniciu, L. *J. Appl. Electrochem.* **1997**, *27*, 875–889.
(26) Sanchez-Sanchez, C. M.; Montiel, V.; Tryk, D. A.; Aldaz, A.; Fujishima, A. *Pure App. Chem.* **2001**, *73*, 1917–1927.
(27) Azuma, M.; Hashimoto, K.; Hiramoto, M.; Watanabe, M.; Sakata, T. *J. Electrochem. Soc.* **1990**, *137*, 1772–1778.

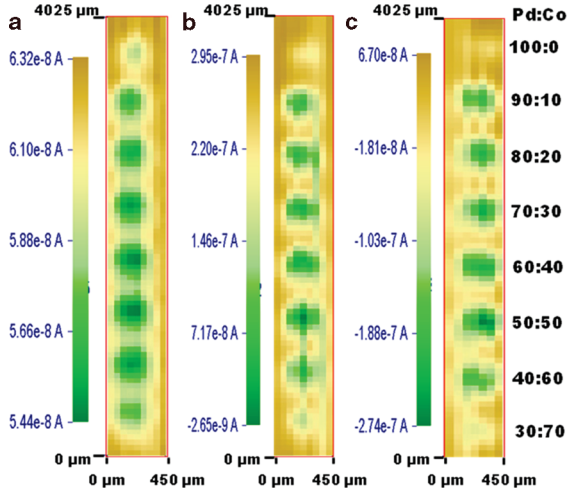

Figure 4. Formic acid oxidation SECM images of a Pd−Co electrocatalyst array at (a) −0.1 V, (b) 0.0 V, and (c) 0.1 V in 0.1 M $KHCO_3$ saturated with CO_2. The tip-substrate distance was 50 μm. The scan rate was 250 μm/s. Tip potential −1.9 V.

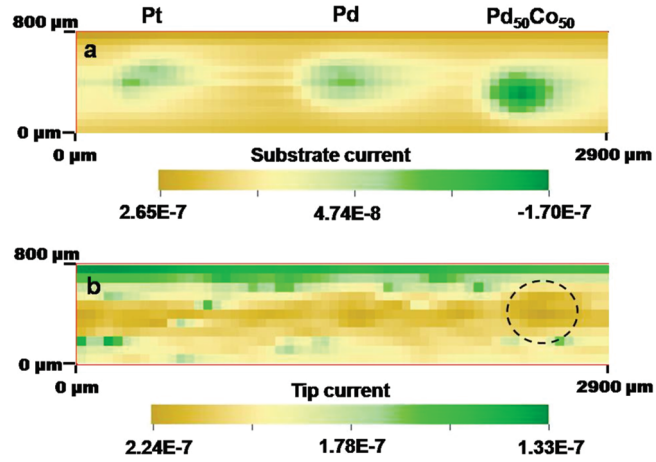

Figure 5. Formic acid oxidation SECM images of Pt, Pd, and $Pd_{50}Co_{50}$ spots at 0.1 V in 0.1 M $KHCO_3$ saturated with CO_2, where (a) is the substrate current and (b) is the tip current. The tip-substrate distance was 50 μm. The scan rate was 250 μm/s and tip potential −1.9 V.

Figure 4 shows the SECM images of formic acid oxidation activity on a Pd−Co electrocatalyst array at different substrate potentials. All three SECM images displayed in Figure 4 show a small reduction background current because of the contribution of the large glassy carbon plate to the overall current. But either a decrease in the positive background current value (Figure 4(a)) or a net oxidation current (Figures 4(b) and (c)) appear when the tip generator is scanned above an active spot for formic acid oxidation. Electrocatalytic activity toward formic acid oxidation could be observed at all Pd−Co spots when the substrate was held at −0.1 V (Figure 4(a)), but the current response at the pure Pd spot was apparently smaller than at all of the other spots. When the substrate potential was held at 0.0 or 0.1 V (Figures 4(b) and (c)), the magnitude of the formic acid oxidation currents were greatly increased compared to those at −0.1 V. The highest formic acid oxidation current was observed at the electrocatalyst spot with the atomic ratio of Pd/Co = 50:50 ($Pd_{50}Co_{50}$), which was distinctly larger than that on the pure Pd spot over the whole potential range studied.

Pt is also known as an active electrocatalyst for formic acid oxidation, but it is poisoned severely by the adsorbed CO formed during the reaction.[28,11] For comparison, a small array with Pt, Pd, and $Pd_{50}Co_{50}$ electrocatalyst spots was prepared, and the formic acid oxidation SECM image at 0.1 V was recorded. As shown in Figure 5(a), the formic acid oxidation current at a $Pd_{50}Co_{50}$ spot was higher than that of the Pt or Pd spots. According to the SECM imaging results, $Pd_{50}Co_{50}$ shows better electrocatalytic activity toward formic acid oxidation than pure Pd or Pt. The results displayed in Figure 4 that show maximum activity at the $Pd_{50}Co_{50}$ spot were obtained in duplicate experiments using different catalyst arrays.

Observation of Positive Feedback at the Hg on Au UME Tip during SECM Imaging. Formic acid oxidation generally follows the so-called "dual-pathway" mechanism involving both a dehydrogenation process leading to direct formation of CO_2 and a dehydration process forming CO, which is further oxidized to CO_2 as an end product.[1,10,28] Thus, it is possible for the CO_2 that is generated at the substrate upon oxidation of formic acid to diffuse back to the tip and contribute additionally to its current, which is always cathodic. This is well-known in SECM as positive feedback[29] and is typically observed for well behaved redox couples (mediators), that is, those that are chemically and electrochemically reversible, stable, and engaged in outer-sphere electron transfers at the electrode. Figure 5(b) shows the reduction current recorded at the Hg on Au UME tip during SECM imaging of Pt, Pd, and $Pd_{50}Co_{50}$ electrocatalyst spots. Such enhancements in the tip cathodic currents that we identify as positive feedback were observed especially when the tip was scanned across the $Pd_{50}Co_{50}$ spot. Our group has previously reported examples in which a catalytic reaction yields a measurable signal coming from a partial positive feedback[30] or positive feedback coming from the interaction of a mediator with a catalytically generated surface species,[31] not so however during imaging in the TG-SC mode. This is because most TG-SC studies are done by galvanostatic (constant current) control of the tip. In this study, the potentiostatic control of the tip allows the feedback loop to be established, resulting in an enhanced contrast during the imaging of the electrochemical activity of the spots (i.e., a larger current gap is observed between active and non-active areas of the array). Furthermore, the observation of this feedback suggests that the main product of the electrocatalytic oxidation of formic acid at the active spots in the substrate is reducible and probably CO_2.

Figure 6 shows the tip and the substrate current responses when performing a line scan in the *x*-direction over the top of a $Pd_{50}Co_{50}$ electrocatalyst spot using a slow scan rate. Anodic and cathodic current responses at the substrate and the tip, respectively, could be recorded at the same time during this line scan. The result strongly suggests that the CO_2 generated

(28) Lu, G.-Q.; Crown, A.; Wieckowski, A. *J. Phys. Chem. B* **1999**, *103*, 9700–9711.
(29) *Scanning Electrochemical Microscopy*; Bard, A. J.; Mirkin, M. V., Eds.; Marcel Dekker: New York, 2001.
(30) Fernandez, J. L.; Hurth, C.; Bard, A. J. *J. Phys. Chem. B* **2005**, *109*, 9532–9539.
(31) Rodríguez-López, J.; Alpuche-Avilés, M. A.; Bard, A. J. *J. Am. Chem. Soc.* **2008**, *130*, 16985–16995.

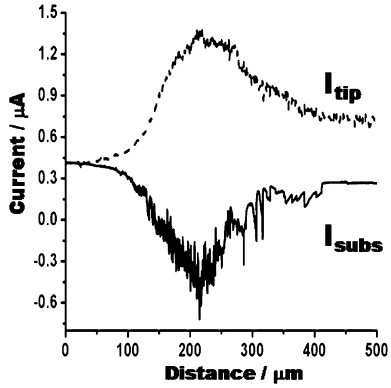

Figure 6. Tip (I_{tip}, dashed line) and substrate (I_{subs}, solid line) current responses when a Hg on Au UME tip was performing CO_2 reduction at −1.9 V and scanned in the *x*-direction (parallel to the substrate) over the top of a $Pd_{50}Co_{50}$ electrocatalyst spot held at 0.1 V. The scan rate was 5 μm/s. Tip−substrate distance was 50 μm.

during the formic acid oxidation at the $Pd_{50}Co_{50}$ substrate forms a supersaturated solution and diffuses to the Hg on Au tip, providing a positive feedback loop, which produces a cathodic current enhancement. This behavior verifies the one previously observed in the tip during SECM imaging (Figure 5(b)). The large enhancement of the cathodic current at the Hg on Au tip is shown in Figure 6 compared to the 150 nA current displayed in Figure 2b in the absence of a feedback reaction.

Cyclic Voltammograms of Formic Acid Oxidation Reaction. Figure 7 shows the cyclic voltammograms for the oxidation of formic acid on Pt, Pd, and $Pd_{50}Co_{50}$ spots in 0.1 M $KHCO_3$ solution containing 10 mM HCOOH, scanning from −0.4 V to more positive values. The observed electrochemical behavior for these catalysts matches the one seen on polycrystalline Pt in sulfuric acid solutions,[28] despite the fact that our measurements are made in a slightly basic medium and thus there is a potential shift of the current responses because of the different pH environment. In the anodic potential scan, the oxidation of formic acid on Pd and $Pd_{50}Co_{50}$ shows broadened current humps between −0.4 to 0.4 V (Figures 7(b) and (c)); the active potential range for formic acid oxidation on Pt only goes between −0.1 and 0.4 V (Figure 7(a)). The onset potential of formic acid oxidation on Pd and $Pd_{50}Co_{50}$ appears about 400 mV earlier than that on Pt. The oxidation current of formic acid at low overvoltage potentials such as −0.1 V is 50% larger on $Pd_{50}Co_{50}$ than on Pd, which agrees with SECM imaging results (Figure 4a). Because the fabrication procedure for the spots involved equimolar amounts of metals deposited for each spot, it is reasonable to assume that the activity of $Pd_{50}Co_{50}$ is better than that of Pd and Pt in terms of the current intensities observed. Moreover, this proves the utility of the SECM screening technique to find higher performance and cheaper catalyst candidates for formic acid oxidation.

CONCLUSIONS

We present a new SECM screening method for the investigation of the activity toward formic acid oxidation of electrocatalysts in 0.1 M $KHCO_3$ solution. An advantageous feature of this SECM screening method compared to non-combinatorial ones is the rapid activity evaluation of a series of bimetallic electrocatalysts with different compositions. In particular, we have

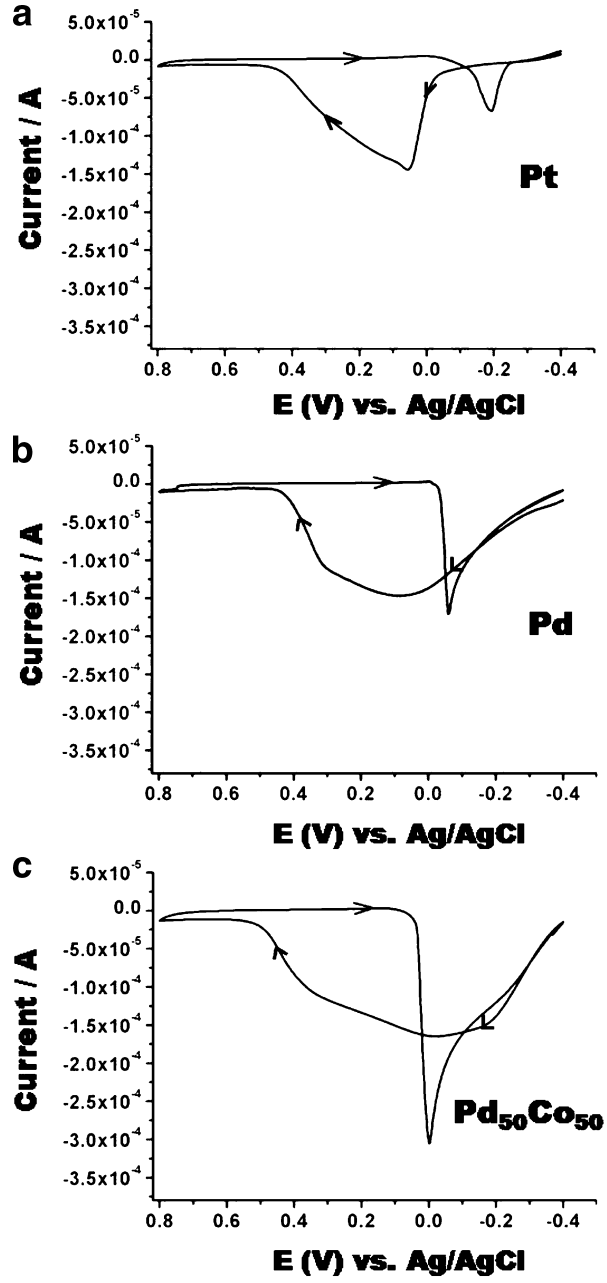

Figure 7. Cyclic voltammograms of the formic acid oxidation at (a) Pt, (b) Pd, and (c) $Pd_{50}Co_{50}$ electrocatalysts in 0.1 M $KHCO_3$ solution containing 10 mM HCOOH. The scan rate was 50 mV/s.

evaluated nine different Pd−Co compositions and three pure metals (Pd, Pt and Co) using this SECM screening method. We found that $Pd_{50}Co_{50}$ performed as a better electrocatalyst toward formic acid oxidation than all the other Pd−Co combinations, pure Pd and Pt. The observation of positive feedback current in the SECM measurements for this material suggest chemical reversibility of the $HCOOH/CO_2$ couple under these conditions, which points toward direct dehydrogenation as the main pathway during formic acid oxidation. Moreover, on the technical side, the positive feedback provides a higher contrast in the SECM image. The observations made with the SECM were further confirmed by traditional cyclic voltammetry experiments, which proved that the SECM screening method is applicable for the screening of new formic acid oxidation electrocatalysts in slightly basic solution. This

TG-SC technique cannot be used in acidic solutions, however, because of the low current efficiency for CO_2 reduction under these conditions. However alternative methods of SECM screening are available for these conditions, as will be described in studies of methanol oxidation.

ACKNOWLEDGMENT

Fellowship support for Changhoon Jung was provided by the Korea Research Foundation funded by the Korean Government (KRF-2007-357-C00073). C. M. Sánchez-Sánchez thanks the Ministerio Español de Educación y Ciencia and Fundación Española para la Ciencia y la Tecnología for a postdoctoral fellowship. J. Rodríguez-López thanks the complementary scholarship support granted by the Secretaría de Educación Pública of Mexico and the Mexican Government. We gratefully acknowledge support from the Robert A. Welch Foundation (F-0021) and the National Science Foundation (CHE-0808927).

Received for review May 19, 2009. Accepted July 4, 2009.

AC901096H